Eur. Phys. J. Plus (2022) 137:1357
https://doi.org/10.1140/epjp/s13360-022-03515-8

THE EUROPEAN PHYSICAL JOURNAL PLUS

Review

Modelling photoevaporation in planet forming discs

Barbara Ercolano[a], **Giovanni Picogna**[b]

Universitäts-Sternwarte, Ludwig-Maximilians-Universität München, Scheinerstr. 1, 81679 Munich, Bayern, Germany

Received: 19 July 2022 / Accepted: 18 November 2022

Abstract Planets are born from the gas and dust discs surrounding young stars. Energetic radiation from the central star can drive thermal outflows from the discs atmospheres, strongly affecting the evolution of the discs and the nascent planetary system. In this context, several numerical models of varying complexity have been developed to study the process of disc photoevaporation from their central stars. We describe the numerical techniques, the results and the predictivity of current models and identify observational tests to constrain them.

1 Introduction

The formation and evolution of planetary systems is strongly coupled to the evolution and final dispersal of the protoplanetary discs in which they form. This is driven to a large extent by irradiation from the central star, which provides heating, ionisation (thus magnetic field coupling) and can trigger thermal outflows that disperse the disc material.

The dispersal of the gas disc imposes a final timescale within which giant planets must form and is of crucial importance for the final architecture of planetary systems. Photoevaporation operates by first opening a gap in the disc, which allows the inner disc to drain onto the central star, while the outer disc is dispersed from the inside out. This provides a natural parking mechanism for migrating planets [1–4] as well as influencing the post-disc dynamical evolution of the orbits [5, 6]. The final distribution of the semi-major axis of giant planets in a population is extremely sensitive to the mass-loss profile of the disc [2, 3].

The role of photoevaporation in the early phases of planet formation, e.g. the formation of planetesimals by the streaming instability is instead debated [7, 8]. For the streaming instability to occur, a high solid-to-gas ratio is needed. Photoevaporation is usually invoked as a mechanism that preferentially removes gas, thus helping to locally increase the dust-to-gas ratio. While [7] test this hypothesis and find that the effect of photoevaporation on the total planetesimal mass is negligible, the opposite conclusion is obtained by [8], using a similar method. The reason for this discrepancy lies in the different photoevaporation mass-loss profiles assumed in these two different works.

Realistic mass-loss profiles are also a key ingredient in planet and disc population synthesis models (e.g. [9–11]), while a reliable disc surface density evolution consistent with the thermodynamical wind structure is crucial for the interpretation of observations of transition discs [12–15] and gas emission lines and dust observation [16–20].

In this context, several theoretical and numerical models of the photoevaporation process in planet-forming discs have been developed over the years, having as the main objective the determination of accurate spatially resolved mass-loss rates.

Recent theoretical and observational advancements (see reviews [21, 22]) which point to disc winds of magnetic nature (MHD winds) in addition to thermal (photoevaporative) winds have added to the urgency of developing quantitatively predictive thermal wind models in order to distinguish them in the observations [18, 23]. This is of paramount importance to assess the relevance of MHD winds to angular momentum extraction from discs.

In this paper, we will review the current stand of numerical photoevaporation models. Special attention will be given to the applicability of the different models, as well as to the divergence of the results. Present and future observational tests of the models are also reviewed.

Focus Point on Environmental and Multiplicity Effects on Planet Formation. Guest editors: G. Lodato, C.F. Manara.

[a] e-mail: ercolano@usm.lmu.de (corresponding author)
[b] e-mail: picogna@usm.lmu.de

Published online: 19 December 2022

2 Numerical modelling

Disc photoevaporation is a coupled problem in radiative transfer, thermochemistry, hydrodynamics and dust dynamics. Until recently, it was deemed impossible to combine all these effects into comprehensive numerical simulations, but in recent years, it has been shown that the codes and numerical capabilities are available [24, 25], though still with significant limitations in the radiative transfer. Theoretical photoevaporation models have been developed for one or a combination of three different portion of the stellar spectra that are capable of driving a disc thermal wind: the far-UV (FUV) 6 eV $< h\nu <$ 13.6 eV; extreme-UV (EUV), 13.6 eV $< h\nu <$ 100 eV; and X-rays, 100 eV $< h\nu <$ 10 keV (in particular its soft component 100 eV $< h\nu <$ 1 keV). Each of them presents its characteristic features and numerical challenges, so it is important to distinguish between them.

EUV radiation

EUV photons are defined as energetic enough to ionise atomic hydrogen from its atomic state ($h\nu > 13.6$ eV). Since the ionisation cross section for neutral hydrogen is $10^{-17}\mathrm{cm}^2\mathrm{atom}^{-1}$, an EUV photon will be absorbed after passing a neutral column density of $N_H = 10^{17}\,\mathrm{cm}^{-2}$. The interaction between a EUV photon and a hydrogen atom is straightforward. The photon is absorbed, producing an ionised hydrogen atom and thermal energy. Typical temperatures in ionised regions are $\sim 10^4$ K. The production of the electron-ion pair is offset by recombinations. Those to the electronic ground state produce a photon with energy larger than 13.6 eV which can further ionise the medium, producing a diffuse field. The recombinations to an excited state instead lead to the destruction of the ionising photon. In the case of irradiation by a central star of a primordial disc with typical scale heights, photons from the central star generate a hot hydrostatic atmosphere of $\sim 10^4$ K above the inner disc. It is then the diffuse field of recombination photons from this atmosphere that irradiates and ionises the outer disc. This problem has to be solved as a 2D radiative transfer, which takes into account the direct and diffuse ionising fields while solving the photoionisation problem.

FUV radiation

FUV photons have energies in the range of 6–13.6 eV, they cannot ionise hydrogen, but they effectively photodissociate molecular hydrogen, CO, and other molecules, and ionise carbon. Photoelectric heating from dust grains and polycyclic aromatic hydrocarbons (PAHs) is the dominant gas heating mechanism for FUV photons. Heating is proportional to the grain surface, thus in the presence of abundant small grains or PAHs in the disc atmosphere, FUVs can heat the gas and potentially contribute to driving a thermal wind [26]. The gas radiates only less than 1% of the energy processed by the dust, and it is heated mainly collisionally by photoelectrons from small dust grains and PAHs, or by vibrationally excited H2. Thus, its temperature is impacted by both dust evolution and chemistry [24, 27]. FUV photons can heat a primarily neutral layer of H and H_2 to temperatures of order 10–5000 K, depending on the magnitude of the flux, the density of the gas, and the chemistry. In order to correctly model this problem, one has to combine a 2D radiative transfer, with a sufficiently large chemical network to account for the strong variation in density and temperature, and a proper dust evolution model. Another complication arises from the fact that the component of the stellar FUV field due to accretion onto the central star can dominate over the chromospheric component. This means that the FUV flux reaching the disc, and thus the wind mass-loss rates, strongly depend on the accretion rate which decreases with time and can stop completely once an inner cavity is formed.

X-ray radiation

X-rays can be divided into two main components: the soft X-rays (100 eV $< h\nu <$ 1 keV), which are absorbed at a column density of $\sim 10^{22}$ pp/cm^2, heating up the disc's upper layers where they drive a thermal wind; the hard X-rays (1 keV $< h\nu <$ 10 keV), which reach much deeper into the disc where dust and gas are thermally coupled, but they can increase the level of ionisation (together with cosmic rays) close to the disc mid-plane thus affecting the coupling of the gas with the disc magnetic field. The main interaction of X-ray photons is via photoionisation of (the inner shells of) atoms and molecules, which can lead to secondary ionisations (including of Hydrogen), followed by the thermalisation of the kinetic energies of primary and secondary electrons. X-ray heating produces a range of temperatures going from a few hundred K in the dense X-ray PDRs up to 10^4 K in the disc upper layers. X-ray luminosities do not depend on stellar accretion rates, and in fact, they remain nearly constant with time during the first Myrs [28], yielding a constant wind mass-loss rate regardless of changes in the surface density of the disc.

2.1 Methods

Since the realisation of the importance of disc photoevaporation, more than 30 years ago [29], the problem has been tackled placing more emphasis either on radiative transfer modelling, or on the full time-dependent radiation hydrodynamics.

The first studies of disc photoevaporation focussed on EUV photoevaporation of discs by OB stars, which are strong EUV emitters. Two lines of models started contemporarily. The first adopting a simplified radiative transfer calculation in the Eddington approximation (reducing the three-dimensional radiative transfer problem to a "three stream" approximation coming from the star, vertically upwards, and downwards at each point in the disc) applied to a vertically hydrostatic disc [30, 31]. The second one, more focused on the dynamics [32, 33], started by developing a 2D hydrodynamic photoionisation code, later improved including the effects of UV dust scattering [34]. Both lines of studies found that the most important contribution to the wind comes from the

diffuse field from a puffed-up bound inner disc and that the thermal wind is launched from the gravitational radius R_g[1] outwards. By adding the analytical prescriptions for mass-loss rates as a function of disc radius due to EUV photoevaporation as a sink term in the 1D disc viscous evolution equation [37, 38], the so-called 'EUV-switch' was demonstrated (see Sect. 3).

The first hydrodynamical models of EUV disc photoevaporation for T Tauri stars [39] were performed assuming an isothermal equation of state and imposing the density at the base of the flow from previous results [31]. They found that the photoevaporative flow was launched subsonically ($\sim 0.3\,c_s$) from a much smaller radius than the gravitational radius ($R_c \simeq R_g/5$) (see also, [36]), which was not expected from the analytical prescription.

These studies were then followed by the first hydrostatic models of X-ray irradiation from T Tauri stars, first with a simple heating model [40], and later with a more realistic two-dimensional Monte Carlo photoionisation and dust radiative transfer code [41, 42]. The latter calculations used a more realistic input spectrum which included both the EUV and X-ray components, showing that the latter completely dominates, with mass-loss rates some two orders of magnitude higher than previous pure EUV models.

At the same time, a 1 + 1D hydrostatic equilibrium model was also developed including EUV, X-rays and FUVs, and a comprehensive chemical network [26, 43]. These models showed that FUV radiation might be efficient at removing material from the outer disc, but only if PAHs are abundant in discs. The input spectrum used by these models was however very idealised, with a hard X-ray input spectrum, which was inefficient at heating the gas and driving the wind.

Without proper hydrodynamical calculations, all these models estimated local mass-loss rates by assuming that the local mass loss rate is roughly equal to the product of the density at the sound speed at the base of the wind, the so-called $\rho \dot{c_s}$ method. Without hydrodynamics, identifying the base of the wind is rather arbitrary and different authors used different approaches, which further exacerbated tension between the models.

The first (radiation-)hydrodynamical calculation including both X-rays and EUV radiation [44, 45] was performed using a parameterisation of gas temperature as a function of the ionisation parameter obtained from detailed thermal and ionisation calculations [42] performed with the MOCASSIN code [46–48]. The ionisation parameter is defined as $\xi = \frac{L_X}{nr^2}$, where L_X is the X-ray luminosity, r and n are the local disc radius and the volume density of the gas. This method is generally known as the $\xi - T_e$ approach. These studies were later extended adopting the modern hydrodynamical code PLUTO [49], and better accounting for attenuation effects in the disc using a column density dependant $\xi - T_e$ parameterisation [50–53]. With this improved prescription it was shown that the X-ray irradiation could reach several hundred au, and that the mass-loss rates for high X-ray luminosities reaches a plateau as more energetic photons cannot heat up lower and denser cold regions of the disc.

The advantage of the $\xi - T_e$ method is that while being based on detailed multi-frequency thermal calculations introduces very little computational overheads on the hydrodynamics. A drawback of this method is that the thermal calculations are performed in radiative equilibrium, and thus the contribution of adiabatic cooling cannot be accounted for. All models performed with the $\xi - T_e$ approach should therefore perform a-posteriori check to ensure that radiative equilibrium is justified throughout the simulation domain. This has indeed been demonstrated for all the models obtained with this approach so far [44, 50–53].

Recently some numerical experiments have been carried out to perform (a very streamlined) radiative transfer and thermochemical calculation on the fly in hydrodynamical models [24, 25]. Due to the high computational costs of this approach, only a handful of models exist with limited spectral and spatial resolution. The results obtained by these models diverge strongly from those obtained with the $\xi - T_e$ method, as discussed in Sect. 3.1.

3 Results

The main results from all photoevaporation models developed to date can be roughly summarised as follows: Radiation from the central star heats the upper layers of protoplanetary discs, which become unbound and are centrifugally accelerated in a thermal outflow. Wind mass-loss rates peak around a specific radius of the disc known as the gravitational radius, with profiles that can be more or less extended to larger radii. No mass-loss is expected to occur from regions that are close to the star, and thus more gravitationally bound, which would require the gas to achieve very high temperatures to escape. The combination of steady mass-loss rates due to photoevaporation and a steadily decreasing accretion rate with time in a viscously accreting disc produces the so-called photoevaporation switch: Discs evolve viscously for a few million years, or until the viscous accretion rate has reached values comparable to the wind mass-loss rate, at which point photoevaporation takes over and the disc is quickly dispersed from the inside out, via the formation of a gap first and then a clear-out cavity.

Modern hydrodynamical models of photoevaporation are performed (at least) in 2D (but see, [54], for 3D simulations including planets) and thus allow only to model the disc for a limited amount of orbits, over which a steady-state solution for the outflow is (ideally) achieved. Modelling the evolution of the surface density of the disc as the gap opens and the disc is dispersed is generally well-beyond feasibility for 2D hydrodynamical calculations. What is done instead is to use the 2D steady-state solution to determine

[1] The gravitational radius is defined as the location where a gas parcel becomes unbound from the central star [31, 35] $R_g = GM_\star/c_s^2$. For gas at roughly 10,000 K in the atmosphere of a disc around a solar mass star this is roughly 5 au. The wind however is launched at the so-called critical radius $R_c \sim 0.2R_g \sim 1$ au (e.g. [36]).

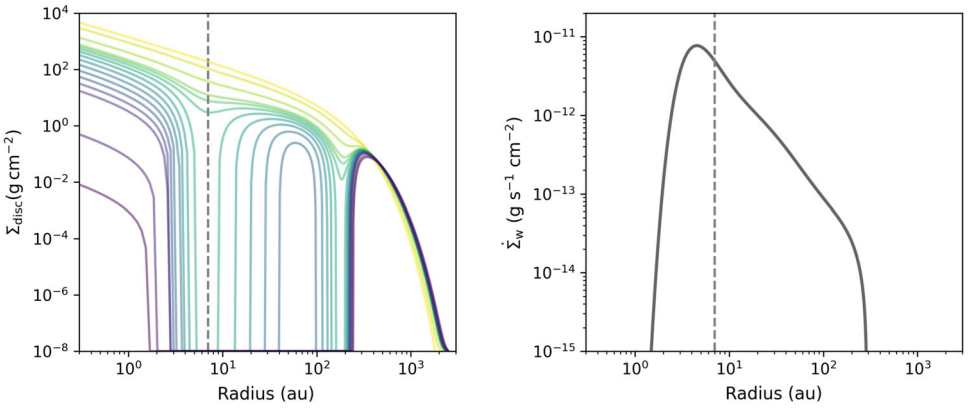

Fig. 1 On the left panel, the 1D surface density evolution as a function of disc radius is shown for a disc of $M_d = 0.1 M_\odot$, orbiting a Solar mass star, with $L_X = 2.04 \times 10^{30}$ erg s^{-1} [52]. The different lines are drawn at [0, 25, 50, 60, 62, 64, 66, 68, 70, 72, 74, 76, 78, 80, 90, 99]% of the corresponding total disc lifetime. The dotted line shows the approximate location of the inner gap opening due to photoevaporation. On the right panel, the corresponding surface density mass-loss rate due to photoevaporation is shown as a function of disc radii

a one-dimensional mass-loss profile, $\dot{\Sigma}_{\rm w}(R)$ [37, 38, 55, 56], which is then included as a sink term to the one-dimensional disc viscous evolution equation [57, 58] to study the surface density evolution of the disc as a function of time:

$$\frac{\partial \Sigma}{\partial t} = \frac{1}{R}\frac{\partial}{\partial R}\left[3R^{1/2}\frac{\partial}{\partial R}\left(\nu \Sigma R^{1/2}\right)\right] - \dot{\Sigma}_{\rm w}(R,t). \tag{1}$$

Figure 1 shows the mass-loss profile for a 1 $M_\odot$ (right panel [52]) and the corresponding surface density evolution (left panel). The surface density evolution (time and location of gap opening, dispersal timescale, etc.) is extremely sensitive to $\dot{\Sigma}(R)$, which in turn affects also the final architecture of planets formed in the disc [1–3], as well as the potential of photoevaporation of triggering the formation of planetesimals by the streaming instability [7, 8].

3.1 Divergence of the results

While the broad-brush picture described above is shared by most authors, the $\dot{\Sigma}_{\rm w}(R)$, and the physical properties of the wind derived by different projects (e.g. see Table 1) diverge significantly. A recent comparison of the surface density mass-loss between the different models of disc photoevaporation (see their Figure 7, [22]) has highlighted an order of magnitude difference in the cumulative mass-loss rates which depends not only on the location of the surface mass-loss rate maximum, but also on the extent of the profiles. These differences can be broadly understood looking at the choices made for the frequency range adopted for the stellar irradiation, and the different methods used. However, most of them present a peak inside 10 au and a slow decline of the surface density mass-loss rate in the outer regions.

As photoevaporation is driven by stellar irradiation, a large part of the divergence can be understood by considering the input spectrum assumed by different authors (see also discussion in [59], section 4.3.1). A pure EUV model (e.g. [60, 61]) yields an almost isothermal gas with a temperature around 10^4 K. In this case, the mass-loss peaks around the gravitational radius which is about 9 au for a 1 $M_\odot$ star, the total mass-loss scales as the square root of the EUV flux, and it is roughly 10^{-10} $M_\odot$/yr assuming a EUV flux of 10^{41} phot/s [60, 61].

Soft X-ray radiation penetrates deeper in the disc than EUV radiation and yields mass-loss rates that are one or two orders of magnitude higher than the classical EUV model, depending almost linearly on the X-ray luminosity of the irradiating star [45, 50, 52]. X-ray photoevaporation models, all include a EUV component, but find it is irrelevant to driving the wind (e.g. [42]). Models for 1 $M_\odot$ star yield total mass-loss rates of order 10^{-8} $M_\odot$/yr assuming a soft spectrum and X-ray luminosities of 10^{30} erg/s [44, 50]. The X-ray-driven mass-loss profile is much more extended than in the EUV case, peaking around the gravitational radius, but extending out to $\sim$ 200 au. Carbon is one of the major contributors in the X-ray opacity, since X-ray photons are mainly absorbed by the inner shells of the more abundant heavy elements in the gas and dust [62]. Carbon depletion is expected as a natural consequence of disk evolution both chemical as the carbon turns from CO into more complex species, and physical due to grain growth that locks up large fractions of carbon in ice bodies. For carbon-depleted disks, the magnitude and extent of the mass-loss rates are expected to increase by a factor $\sim$ 2 [51]. Internal FUV radiation is expected to drive photoevaporation from further out in the disc, and initial estimates, based on the hydrostatic equilibrium models of [26], found it to be very efficient under the assumption that polycyclic aromatic hydrocarbons (PAHs) are abundant in the atmosphere of discs. However, the atmospheric abundance of PAHs, which are rarely observed in T Tauri discs [63], is likely to be very small, furthermore stellar FUV flux depends on the accretion rate onto the central star and decreases with time. For these reasons, the role of FUV-driven winds on the final disc dispersal is uncertain.

More recent calculations [25], while considering EUV, FUV and X-ray simultaneously, come to the conclusion that *direct* EUV flux dominates the driving of the wind, but obtain two orders of magnitude higher mass-loss rates than previous EUV-only models. These calculations are in direct contrast with the classical picture that stellar (direct) EUV photons are absorbed in the bound inner regions of the disc, and the diffuse field coming from the puffed-up inner disc drives photoevaporation (at low rates) at the gravitational radius. The assumption that direct EUV are able to reach the disc at and beyond the gravitational radius relies on

Table 1 Model comparison

Project	Hydro	Dust	Radiation	Chemistry	Spectrum
Wang et al.[1]	Yes	$r_{\rm dust}$: 5 Å d/g: 7×10^{-5} *no dynamics/growth*	Yes *ray-tracing* *(no diffuse field)*	24 species of H,He,C,O,S, Si,Fe,dust grains,e^-, $\sim$ 100 chemical reactions	4 energy bins: 7 eV (FUV), 12 eV (L–W), 25 eV (EUV), and 1 keV (X-ray band)
Nakatani et al.[2]	Yes	MRN (3.1 Å$\rightarrow$ 0.01μm) d/g: $10^{-6} \rightarrow 10^{-1}$ *no dynamics/growth*	Yes *ray-tracing* *(no diffuse field)*	8 species of H,C,O, grains 13 chemical reactions	81 freq. bins for FUV/EUV X-ray SED derived from TW-Hya
$\xi - T_e$ Approach[3]	Yes	MRN (50 Å$\rightarrow$ 0.25 μm) d/g: $2.5, 4 \times 10^{-4}$ *no dynamics/growth*	Yes *Monte Carlo RT* *(radiative equilibrium)*	No	$>$ 1000 freq. bins *obs. derived input spectra* *different spec. hardness*
Gorti et al.[4]	No *vertical hydrostatic equilibrium*	MRN (50 Å$\rightarrow$ 20 μm) d/g: 0.01 *no dynamics/growth*	Yes *1+1D gas and dust radiative transfer*	84 species of H, He, C, O, Ne,S, Mg, Fe, Si, Ar, S, Mg, Fe, Si, Ar, $\sim$ 600 chemical reactions	$L_X(E) \propto E\,[0.1-2]$ keV $L_X(E) \propto E^{-1.75}$ $[2-10]$ keV
Ercolano et al.[5]	No *vertical hydrostatic equilibrium*	MRN (50 Å$\rightarrow$ 0.25 μm) d/g: $2.5, 4 \times 10^{-4}$ *no dynamics/growth*	Yes *full Monte Carlo RT* with dust and gas	Atomic and photoionised species of H, He, C, O, Ne, S, Mg, Fe, Si, Ar	$>$ 1000 freq. bins, *obs. derived input spectrum*
Alexander et al.[6]	Yes		No	No	–

[1][24, 99], [2][25, 101, 102], [3][44, 45, 50–53], [4][26], [5][42], [6][60, 61]

previous calculations [64]. The source of the discrepancy between these more recent calculations and previous works might lie in the specific disc geometries assumed, where the inner disc does not expand enough to screen the outer regions or where there is significant flaring, which might not apply to the majority of discs [65]. We finally note that these results are also in tension with previous work [42] which by means of detailed 2D Monte Carlo RT and thermal calculation in a hydrostatic disc, explicitly test the role of EUV in the presence of an observationally derived X-ray spectrum and find EUV effects to be negligible on the final mass-loss rates. A detailed comparison in a dedicated work must however be carried out to finally determine the nature of this discrepancy.

Strong divergence is also observed in the physical properties of the wind obtained by recent calculations [24] which use the ATHENA++ code [66, 67] to perform self-consistent radiation hydrodynamics and thermochemical calculation of photoionised disc compared to models that use the $\xi - T_e$ approach [44, 45, 50, 52, 53]. While total mass-loss rates obtained are comparable, the ATHENA++ models come to the conclusion that X-ray radiation is inefficient at driving the wind and that EUV dominates. Also the temperature structure of the wind is significantly different in the two cases. The ATHENA++ models predict extremely high temperatures (10^5 K) at the base of the wind which decreases higher up, in contrast with the Parker-like wind obtained by the $\xi - T_e$ models, which has a few 10^3 K launching temperature and reaches top temperatures of 10^4 K but only for the very limited region of the wind that is heated (not launched!) by EUV radiation. The divergence of these models has been often attributed to methodological differences on how to approach to radiative transfer and thermal balance, the choice of irradiating spectrum employed, and the processes available to cool the gas. A recent detailed comparison [68] has been able to shed light on this question, demonstrating that the divergence between these models is driven predominantly by the choice of the irradiating spectrum and the very limited number of frequency points used to describe the radiation field by the ATHENA++ model (7) compared to the $\xi - T_e$ models (>1000). The $\xi - T_e$ models use an X-ray spectrum derived from deep Chandra observations of T Tauri stars [41, 53, 69], while the ATHENA++ model assumes an analytical distribution.

4 Observational tests

For complex theoretical models to become a realistic description of natural phenomena rather than remaining numerical experiments, it is very important that they provide predictions that can be tested against observations. In this section, we list a number of direct and indirect tests that have been used to constrain theoretical photoevaporation models.

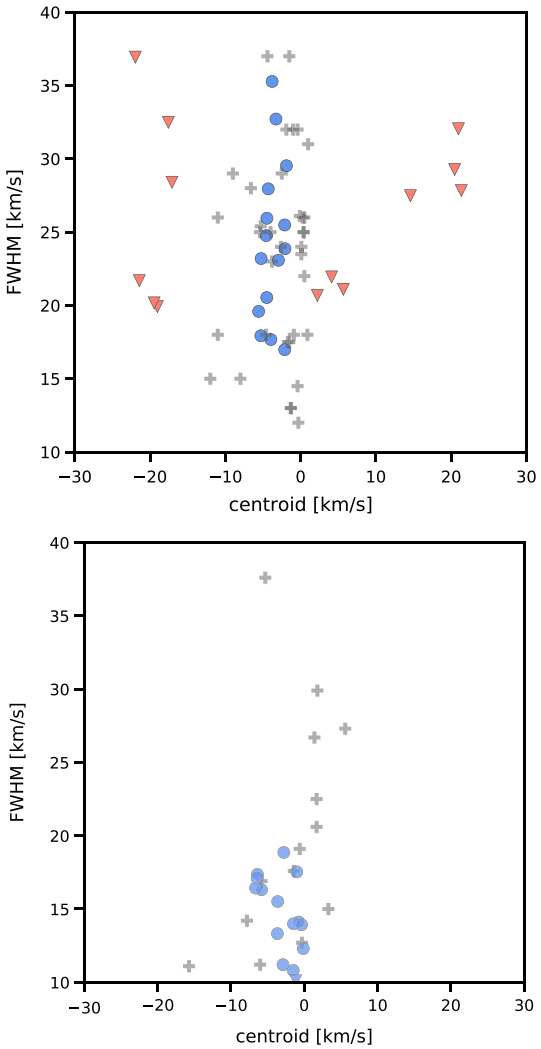

Fig. 2 Left Panel: Full width at half maximum versus peak velocity of the narrow low-velocity components (NLVC) which result from the multi-Gaussian decomposition of [OI] 6300 Å line profiles. Grey plusses mark the observed NLVCs [71]. Blue circles and red triangles show NVLCs from the photoevaporation and MHD wind models [18], respectively. Right Panel: Same as figure but for the NLVC of the o−H_2 1−0 S(1) at 2.12 μm. Grey pluses show the observed NLVCs [70]. The blue circles show the results for the same physical photoevaporative wind models as shown in figure, but post-processed with a thermo-chemical code to properly model the molecular hydrogen chemistry and excitation [Rab et al., subm.]

4.1 Direct tests

Winds are tenuous and direct imaging of its gas component is not possible. However, the gaseous component of the wind can still be "observed" directly via high-resolution spectroscopy of emission lines that are emitted in the outflow and show a blue-shifted component [21, 22]. Line profiles of collisionally ionised lines of neutral and low ionisation species ([OI], [NeII], [SII], [N2], [FeII]), as well as some molecular tracers (CO and H_2), are available for a statistically significant number of T Tauri stars (e.g. [70–72]). The majority of the observed profiles can be well-fitted by X-ray-driven photoevaporative models [16, 17, 73], in combination with a magnetically driven component for sources showing composite profiles [18] (see Fig. 2). Lines in the sub-mm region (e.g. CO and CI) have also been used to infer the presence of disc winds in highly inclined sources [74], and some predictions from numerical MHD wind models already exist [75].

Ionised gas in the wind and disc atmosphere region could also be detected and spatially constrained via its free-free emission at cm-wavelengths using observations from upcoming high spatial resolution facilities like ngVLA (e.g. [23]). This is a promising avenue to distinguish magnetic winds which can be driven from regions much closer to the star than photoevaporative winds.

Small ($\lessapprox$ 10 μm) dust grains can be entrained in the wind from the launching region [76–83], and it may be possible to detect their signature in scattered light observations of highly inclined sources, particularly from discs with inner dust cavities [19, 20].

4.2 Indirect tests

Indirect constraints that photoevaporation models should match might include (i) observed disc dispersal timescales which can be traced by the evolution of the accretion properties and surface density of observed disc populations, including during the transition disc phase (e.g. [77, 84–89]); (ii) metallicity dependence of disc lifetimes [25, 62, 90–93]; (iii) observed correlations in disc populations like the $\dot{M} - M_\star$ relation (e.g. [94–96]).

It is important to note that in order to test photoevaporation models against observed disc populations, wind properties (mass-loss rates as a function of disc radius) must be calculated for a wide enough parameter space, spanning the observed stellar masses and X-ray properties. Assumptions are then necessary as to how angular momentum is transported in the disc. Most studies to date have assumed a viscous model in combination with photoevaporation. It would be interesting to repeat this body of work assuming angular momentum transport by magnetised disc winds (e.g. [97, 98]).

5 Outlook

As mentioned at the end of the last section, magnetised disc winds might be present in combination with thermal winds and the former might provide the dominant mechanism for angular momentum transport instead of viscosity. Direct hints of their presence are seen in emission line profiles observed for some sources which show multiple outflow components (e.g. [22], for a recent review). Furthermore, non-ideal magnetohydrodynamical models routinely observe magnetised winds, while they struggle to maintain magnetorotational instability active in most regions of the disc (e.g. [59], for a recent review). Clearly, the frontier of modelling disc winds is to account for both processes simultaneously and at high enough spatial resolution to produce models that have enough predictive power to be confronted with the observations. Initial attempts are promising (e.g. [99, 100]), but they still lack resolution in the inner disc regions (where most observed diagnostics come from), have a large lower density threshold (comparable to the wind density, making post-processing of the winds problematic), oversimplify radiative transfer and rely on a number of unconstrained parameters to describe the magnetic flux and its evolution. If these problems can be overcome, these models could acquire enough predictive power for a meaningful comparison with the observations, as detailed in the previous section, and thus provide us with powerful tools to understand how protoplanetary discs evolve and finally disperse.

Acknowledgements We thank the anonymous referee for a thorough and constructive report that helped improve this review. We acknowledge the support of the Excellence Cluster ORIGINS which is funded by the Deutsche Forschungsgemeinschaft (DFG, German Research Foundation) under Germany's Excellence Strategy—EXC-2094-390783311. BE, GP and CHR acknowledge the support of the Deutsche Forschungsgemeinschaft (DFG, German Research Foundation)—325594231.

Funding Open Access funding enabled and organized by Projekt DEAL.

Data Availability Statement This manuscript has no associated data or the data will not be deposited. [Authors' comment: There are no associated data available.]

References

1. R.D. Alexander, I. Pascucci, Deserts and pile-ups in the distribution of exoplanets due to photoevaporative disc clearing. Mon. Not. RAS **422**(1), 82–86 (2012). https://doi.org/10.1111/j.1745-3933.2012.01243.x. arXiv:1202.5554 [astro-ph.EP]
2. B. Ercolano, G. Rosotti, The link between disc dispersal by photoevaporation and the semimajor axis distribution of exoplanets. Mon. Not. RAS **450**(3), 3008–3014 (2015). https://doi.org/10.1093/mnras/stv833. arXiv:1504.03433 [astro-ph.EP]
3. J. Jennings, B. Ercolano, G.P. Rosotti, The comparative effect of FUV, EUV and X-ray disc photoevaporation on gas giant separations. Mon. Not. RAS **477**(3), 4131–4141 (2018). https://doi.org/10.1093/mnras/sty964. arXiv:1803.00571 [astro-ph.EP]
4. K. Monsch, B. Ercolano, G. Picogna, T. Preibisch, M.M. Rau, The imprint of X-ray photoevaporation of planet-forming discs on the orbital distribution of giant planets. Mon. Not. RAS **483**(3), 3448–3458 (2019). https://doi.org/10.1093/mnras/sty3346. arXiv:1812.02173 [astro-ph.EP]
5. N. Moeckel, P.J. Armitage, Hydrodynamic outcomes of planet scattering in transitional discs. Mon. Not. RAS **419**(1), 366–376 (2012). https://doi.org/10.1111/j.1365-2966.2011.19699.x. arXiv:1108.5382 [astro-ph.EP]
6. B. Liu, S.N. Raymond, S.A. Jacobson, Early solar system instability triggered by dispersal of the gaseous disk. Nature **604**(7907), 643–646 (2022). https://doi.org/10.1038/s41586-022-04535-1. arXiv:2205.02026 [astro-ph.EP]
7. B. Ercolano, J. Jennings, G. Rosotti, T. Birnstiel, X-ray photoevaporation's limited success in the formation of planetesimals by the streaming instability. Mon. Not. RAS **472**(4), 4117–4125 (2017). https://doi.org/10.1093/mnras/stx2294. arXiv:1709.00361 [astro-ph.EP]
8. D. Carrera, U. Gorti, A. Johansen, M.B. Davies, Planetesimal formation by the streaming instability in a photoevaporating disk. Astrophys. J. **839**(1), 16 (2017). https://doi.org/10.3847/1538-4357/aa6932. arXiv:1703.07895 [astro-ph.EP]
9. A. Emsenhuber, C. Mordasini, R. Burn, Y. Alibert, W. Benz, E. Asphaug, The New Generation Planetary Population Synthesis (NGPPS). I. Bern global model of planet formation and evolution, model tests, and emerging planetary systems. Astron. Astrophys. **656**, 69 (2021). https://doi.org/10.1051/0004-6361/202038553. arXiv:2007.05561 [astro-ph.EP]
10. A. Emsenhuber, C. Mordasini, R. Burn, Y. Alibert, W. Benz, E. Asphaug, The New Generation Planetary Population Synthesis (NGPPS). II. Planetary population of solar-like stars and overview of statistical results. Astron. Astrophys. **656**, 70 (2021). https://doi.org/10.1051/0004-6361/202038863. arXiv:2007.05562 [astro-ph.EP]

11. C.F. Manara, A. Morbidelli, T. Guillot, Why do protoplanetary disks appear not massive enough to form the known exoplanet population? Astron. Astrophys. **618**, 3 (2018). https://doi.org/10.1051/0004-6361/201834076. arXiv:1809.07374 [astro-ph.EP]
12. G.P. Rosotti, B. Ercolano, J.E. Owen, The long-term evolution of photoevaporating transition discs with giant planets. Mon. Not. RAS **454**(2), 2173–2182 (2015). https://doi.org/10.1093/mnras/stv2102. arXiv:1509.04278 [astro-ph.EP]
13. J.E. Owen, The origin and evolution of transition discs: successes, problems, and open questions. Publ. Astron. Soc. Aust. **33**, 005 (2016). https://doi.org/10.1017/pasa.2016.2. arXiv:1512.06873 [astro-ph.SR]
14. B. Ercolano, G.P. Rosotti, G. Picogna, L. Testi, A photoevaporative gap in the closest planet-forming disc. Mon. Not. RAS **464**(1), 95–99 (2017). https://doi.org/10.1093/mnrasl/slw188. arXiv:1609.03903 [astro-ph.EP]
15. C. Schaefer, G. Picogna, B. Ercolano, R. Franz, M. Garate, Observability of photoevaporation signatures in the dust continuum emission of transition discs. (in prep) (2022)
16. B. Ercolano, J.E. Owen, Theoretical spectra of photoevaporating protoplanetary discs: an atlas of atomic and low-ionization emission lines. Mon. Not. RAS **406**(3), 1553–1569 (2010). https://doi.org/10.1111/j.1365-2966.2010.16798.x. arXiv:1004.1203 [astro-ph.GA]
17. B. Ercolano, J.E. Owen, Blueshifted [OI] lines from protoplanetary discs: the smoking gun of X-ray photoevaporation. Mon. Not. RAS **460**(4), 3472–3478 (2016). https://doi.org/10.1093/mnras/stw1179. arXiv:1605.04066 [astro-ph.EP]
18. M.L. Weber, B. Ercolano, G. Picogna, L. Hartmann, P.J. Rodenkirch, The interpretation of protoplanetary disc wind diagnostic lines from X-ray photoevaporation and analytical MHD models. Mon. Not. RAS **496**(1), 223–244 (2020). https://doi.org/10.1093/mnras/staa1549. arXiv:2005.14312 [astro-ph.SR]
19. R. Franz, B. Ercolano, S. Casassus, G. Picogna, T. Birnstiel, S. Pérez, C. Rab, A. Sharma, Dust entrainment in photoevaporative winds: densities and imaging. Astron. Astrophys. **657**, 69 (2022). https://doi.org/10.1051/0004-6361/202140812. arXiv:2110.10637 [astro-ph.EP]
20. R. Franz, G. Picogna, B. Ercolano, S. Casassus, T. Birnstiel, C. Rab, S. Pérez, Dust entrainment in photoevaporative winds: synthetic observations of transition disks. Astron. Astrophys. **659**, 90 (2022). https://doi.org/10.1051/0004-6361/202142785. arXiv:2201.12108 [astro-ph.EP]
21. B. Ercolano, I. Pascucci, The dispersal of planet-forming discs: theory confronts observations. R. Soc. Open Sci. **4**(4), 170114 (2017). https://doi.org/10.1098/rsos.170114. arXiv:1704.00214 [astro-ph.EP]
22. I. Pascucci, S. Cabrit, S. Edwards, U. Gorti, O. Gressel, T. Suzuki, The role of disk winds in the evolution and dispersal of protoplanetary disks. arXiv e-prints, 2203–10068 (2022). arXiv:2203.10068 [astro-ph.EP]
23. L. Ricci, S.K. Harter, B. Ercolano, M. Weber, Testing photoevaporation and MHD disk wind models through future high-angular resolution radio observations: the case of TW hydrae. Astrophys. J. **913**(2), 122 (2021). https://doi.org/10.3847/1538-4357/abf5d8. arXiv:2104.03400 [astro-ph.EP]
24. L. Wang, J. Goodman, Hydrodynamic photoevaporation of protoplanetary disks with consistent thermochemistry. Astrophys. J. **847**(1), 11 (2017). https://doi.org/10.3847/1538-4357/aa8726. arXiv:1706.03155 [astro-ph.EP]
25. R. Nakatani, T. Hosokawa, N. Yoshida, H. Nomura, R. Kuiper, Radiation hydrodynamics simulations of photoevaporation of protoplanetary disks by ultraviolet radiation: metallicity dependence. Astrophys. J. **857**(1), 57 (2018). https://doi.org/10.3847/1538-4357/aab70b. arXiv:1706.04570 [astro-ph.EP]
26. U. Gorti, C.P. Dullemond, D. Hollenbach, Time evolution of viscous circumstellar disks due to photoevaporation by far-ultraviolet, extreme-ultraviolet, and X-ray radiation from the central star. Astrophys. J. **705**(2), 1237–1251 (2009). https://doi.org/10.1088/0004-637X/705/2/1237. arXiv:0909.1836 [astro-ph.SR]
27. U. Gorti, D. Hollenbach, C.P. Dullemond, The impact of dust evolution and photoevaporation on disk dispersal. Astrophys. J. **804**(1), 29 (2015). https://doi.org/10.1088/0004-637X/804/1/29. arXiv:1502.07369 [astro-ph.EP]
28. K.V. Getman, E.D. Feigelson, G.P. Garmire, P.S. Broos, M.A. Kuhn, T. Preibisch, V.S. Airapetian, Evolution of X-ray activity in < 25 Myr old pre-main sequence stars. arXiv e-prints, 2203–02047 (2022) arXiv:2203.02047 [astro-ph.SR]
29. J. Bally, N.Z. Scoville, Structure and evolution of molecular clouds near H II regions. II. The disk constrained H II region, S 106. Astrophys. J. **255**, 497–509 (1982). https://doi.org/10.1086/159850
30. D. Hollenbach, D. Johnstone, F. Shu, Photoevaporation of disks around massive stars and ultracompact HH regions. In: J.P. Cassinelli, E.B. Churchwell (eds.) Massive Stars: Their Lives in the Interstellar Medium. Astronomical Society of the Pacific Conference Series, vol. 35, p. 26 (1993)
31. D. Hollenbach, D. Johnstone, S. Lizano, F. Shu, Photoevaporation of disks around massive stars and application to ultracompact H II regions. Astrophys. J. **428**, 654 (1994). https://doi.org/10.1086/174276
32. H.W. Yorke, A. Welz, Formation and early evolution of H II regions. In: Star Formation, Galaxies and the Interstellar Medium, p. 239 (1993)
33. H.W. Yorke, M. Kaisig, Use of multiply nested grids for the solution of flux-limited radiation diffusion and hydrodynamics. Comput. Phys. Commun. **89**(1–3), 29–44 (1995). https://doi.org/10.1016/0010-4655(94)00184-4
34. S. Richling, H.W. Yorke, Photoevaporation of protostellar disks. II. The importance of UV dust properties and ionizing flux. Astron. Astrophys. **327**, 317–324 (1997)
35. K. Liffman, The gravitational radius of an irradiated disk. Publ. Astron. Soc. Aust. **20**(4), 337–339 (2003). https://doi.org/10.1071/AS03019
36. C.P. Dullemond, D. Hollenbach, I. Kamp, P. D'Alessio, Models of the structure and evolution of protoplanetary disks. In: B. Reipurth, D. Jewitt, K. Keil (eds.) Protostars and Planets V, p. 555 (2007)
37. C.J. Clarke, A. Gendrin, M. Sotomayor, The dispersal of circumstellar discs: the role of the ultraviolet switch. Mon. Not. RAS **328**(2), 485–491 (2001). https://doi.org/10.1046/j.1365-8711.2001.04891.x
38. I. Matsuyama, D. Johnstone, L. Hartmann, Viscous diffusion and photoevaporation of stellar disks. Astrophys. J. **582**(2), 893–904 (2003). https://doi.org/10.1086/344638. arXiv:astro-ph/0209498 [astro-ph]
39. A.S. Font, I.G. McCarthy, D. Johnstone, D.R. Ballantyne, Photoevaporation of circumstellar disks around young stars. Astrophys. J. **607**(2), 890–903 (2004). https://doi.org/10.1086/383518. arXiv:astro-ph/0402241 [astro-ph]
40. R.D. Alexander, C.J. Clarke, J.E. Pringle, The effects of X-ray photoionization and heating on the structure of circumstellar discs. Mon. Not. RAS **354**(1), 71–80 (2004). https://doi.org/10.1111/j.1365-2966.2004.08161.x. arXiv:astro-ph/0406643 [astro-ph]
41. B. Ercolano, J.J. Drake, J.C. Raymond, C.C. Clarke, X-Ray-irradiated protoplanetary disk atmospheres. I. Predicted emission-line spectrum and photoevaporation. Astrophys. J. **688**(1), 398–407 (2008). https://doi.org/10.1086/590490. arXiv:0805.4625 [astro-ph]
42. B. Ercolano, C.J. Clarke, J.J. Drake, X-Ray irradiated protoplanetary disk atmospheres. II. Predictions from models in hydrostatic equilibrium. Astrophys. J. **699**(2), 1639–1649 (2009). https://doi.org/10.1088/0004-637X/699/2/1639. arXiv:0905.1001 [astro-ph.GA]
43. U. Gorti, D. Hollenbach, Photoevaporation of circumstellar disks by far-ultraviolet, extreme-ultraviolet and X-ray radiation from the central star. Astrophys. J. **690**(2), 1539–1552 (2009). https://doi.org/10.1088/0004-637X/690/2/1539. arXiv:0809.1494 [astro-ph]
44. J.E. Owen, B. Ercolano, C.J. Clarke, R.D. Alexander, Radiation-hydrodynamic models of X-ray and EUV photoevaporating protoplanetary discs. Mon. Not. RAS **401**(3), 1415–1428 (2010). https://doi.org/10.1111/j.1365-2966.2009.15771.x. arXiv:0909.4309 [astro-ph.SR]
45. J.E. Owen, C.J. Clarke, B. Ercolano, On the theory of disc photoevaporation. Mon. Not. RAS **422**(3), 1880–1901 (2012). https://doi.org/10.1111/j.1365-2966.2011.20337.x. arXiv:1112.1087 [astro-ph.SR]

46. B. Ercolano, M.J. Barlow, P.J. Storey, X.-W. Liu, MOCASSIN: a fully three-dimensional Monte Carlo photoionization code. Mon. Not. RAS **340**(4), 1136–1152 (2003). https://doi.org/10.1046/j.1365-8711.2003.06371.x. arXiv:astro-ph/0209378 [astro-ph]
47. B. Ercolano, M.J. Barlow, P.J. Storey, The dusty MOCASSIN: fully self-consistent 3D photoionization and dust radiative transfer models. Mon. Not. RAS **362**(3), 1038–1046 (2005). https://doi.org/10.1111/j.1365-2966.2005.09381.x. arXiv:astro-ph/0507050 [astro-ph]
48. B. Ercolano, P.R. Young, J.J. Drake, J.C. Raymond, X-ray enabled MOCASSIN: a three-dimensional code for photoionized media. Astrophys. J. Suppl. **175**(2), 534–542 (2008). https://doi.org/10.1086/524378. arXiv:0710.2103 [astro-ph]
49. A. Mignone, G. Bodo, S. Massaglia, T. Matsakos, O. Tesileanu, C. Zanni, A. Ferrari, PLUTO: a numerical code for computational astrophysics. Astrophys. J. Suppl. **170**(1), 228–242 (2007). https://doi.org/10.1086/513316. arXiv:astro-ph/0701854 [astro-ph]
50. G. Picogna, B. Ercolano, J.E. Owen, M.L. Weber, The dispersal of protoplanetary discs—I. A new generation of X-ray photoevaporation models. Mon. Not. RAS **487**(1), 691–701 (2019). https://doi.org/10.1093/mnras/stz1166. arXiv:1904.02752 [astro-ph.EP]
51. L. Wölfer, G. Picogna, B. Ercolano, E.F. van Dishoeck, Radiation-hydrodynamical models of X-ray photoevaporation in carbon-depleted circumstellar discs. Mon. Not. RAS **490**(4), 5596–5614 (2019). https://doi.org/10.1093/mnras/stz2939. arXiv:1910.08565 [astro-ph.EP]
52. G. Picogna, B. Ercolano, C.C. Espaillat, The dispersal of protoplanetary discs—III. Influence of stellar mass on disc photoevaporation. Mon. Not. RAS **508**(3), 3611–3619 (2021). https://doi.org/10.1093/mnras/stab2883. arXiv:2110.01250 [astro-ph.EP]
53. B. Ercolano, G. Picogna, K. Monsch, J.J. Drake, T. Preibisch, The dispersal of protoplanetary discs—II: photoevaporation models with observationally derived irradiating spectra. Mon. Not. RAS **508**(2), 1675–1685 (2021). https://doi.org/10.1093/mnras/stab2590. arXiv:2109.04113 [astro-ph.EP]
54. M. Weber, B. Ercolano, G. Picogna, C. Rab, The interplay between forming planets and photo-evaporating discs I: forbidden line diagnostics. sub. to MNRAS (2022)
55. R.D. Alexander, P.J. Armitage, Giant planet migration, disk evolution, and the origin of transitional disks. Astrophys. J. **704**(2), 989–1001 (2009). https://doi.org/10.1088/0004-637X/704/2/989. arXiv:0909.0004 [astro-ph.EP]
56. K. Monsch, G. Picogna, B. Ercolano, T. Preibisch, The imprint of X-ray photoevaporation of planet-forming discs on the orbital distribution of giant planets. II. Theoretical predictions. Astron. Astrophys. **650**, 199 (2021). https://doi.org/10.1051/0004-6361/202140647. arXiv:2105.05908 [astro-ph.EP]
57. D. Lynden-Bell, J.E. Pringle, The evolution of viscous discs and the origin of the nebular variables. Mon. Not. RAS **168**, 603–637 (1974). https://doi.org/10.1093/mnras/168.3.603
58. J.E. Pringle, Accretion discs in astrophysics. Ann. Rev. Astron. Astrophys. **19**, 137–162 (1981). https://doi.org/10.1146/annurev.aa.19.090181.001033
59. G. Lesur, B. Ercolano, M. Flock, M.-K. Lin, C.-C. Yang, J.A. Barranco, P. Benitez-Llambay, J. Goodman, A. Johansen, H. Klahr, G. Laibe, W. Lyra, P. Marcus, R.P. Nelson, J. Squire, J.B. Simon, N. Turner, O.M. Umurhan, A.N. Youdin, Hydro-, magnetohydro-, and dust-gas dynamics of protoplanetary disks. arXiv e-prints, 2203–09821 (2022). arXiv:2203.09821 [astro-ph.EP]
60. R.D. Alexander, C.J. Clarke, J.E. Pringle, Photoevaporation of protoplanetary discs—I. Hydrodynamic models. Mon. Not. RAS **369**(1), 216–228 (2006). https://doi.org/10.1111/j.1365-2966.2006.10293.x. arXiv:astro-ph/0603253 [astro-ph]
61. R.D. Alexander, C.J. Clarke, J.E. Pringle, Photoevaporation of protoplanetary discs—II. Evolutionary models and observable properties. Mon. Not. RAS **369**(1), 229–239 (2006). https://doi.org/10.1111/j.1365-2966.2006.10294.x. arXiv:astro-ph/0603254 [astro-ph]
62. B. Ercolano, C.J. Clarke, Metallicity, planet formation and disc lifetimes. Mon. Not. RAS **402**(4), 2735–2743 (2010). https://doi.org/10.1111/j.1365-2966.2009.16094.x. arXiv:0910.5110 [astro-ph.EP]
63. J.Y. Seok, A. Li, Polycyclic aromatic hydrocarbons in protoplanetary disks around Herbig Ae/Be and T Tauri stars. Astrophys. J. **835**(2), 291 (2017). https://doi.org/10.3847/1538-4357/835/2/291. arXiv:1612.09454 [astro-ph.SR]
64. K.E.I. Tanaka, T. Nakamoto, K. Omukai, Photoevaporation of circumstellar disks revisited: the dust-free case. Astrophys. J. **773**(2), 155 (2013). https://doi.org/10.1088/0004-637X/773/2/155. arXiv:1306.6623 [astro-ph.SR]
65. D. Hollenbach, The effect of photoevaporation on the first stars. Mem. Soc. Astron. Ital. **88**, 685 (2017)
66. C.J. White, J.M. Stone, C.F. Gammie, An extension of the Athena++ code framework for GRMHD based on advanced Riemann solvers and staggered-mesh constrained transport. Astrophys. J. Suppl. **225**(2), 22 (2016). https://doi.org/10.3847/0067-0049/225/2/22. arXiv:1511.00943 [astro-ph.HE]
67. J.M. Stone, K. Tomida, C.J. White, K.G. Felker, The Athena++ adaptive mesh refinement framework: design and magnetohydrodynamic solvers. Astrophys. J. Suppl. **249**(1), 4 (2020). https://doi.org/10.3847/1538-4365/ab929b. arXiv:2005.06651 [astro-ph.IM]
68. A.D. Sellek, C.J. Clarke, B. Ercolano, The importance of X-ray frequency in driving photoevaporative winds. Mon. Not. RAS **514**(1), 535–554 (2022). https://doi.org/10.1093/mnras/stac1148. arXiv:2204.09704 [astro-ph.EP]
69. K.V. Getman, E. Flaccomio, P.S. Broos, N. Grosso, M. Tsujimoto, L. Townsley, G.P. Garmire, J. Kastner, J. Li, J.F.R. Harnden, S. Wolk, S.S. Murray, C.J. Lada, A.A. Muench, M.J. McCaughrean, G. Meeus, F. Damiani, G. Micela, S. Sciortino, J. Bally, L.A. Hillenbrand, W. Herbst, T. Preibisch, E.D. Feigelson, Chandra Orion ultradeep project: observations and source lists. Astrophys. J. Suppl. **160**(2), 319–352 (2005). https://doi.org/10.1086/432092. arXiv:astro-ph/0410136 [astro-ph]
70. M.N. Simon, I. Pascucci, S. Edwards, W. Feng, U. Gorti, D. Hollenbach, E. Rigliaco, J.T. Keane, Tracing slow winds from T Tauri stars via low-velocity Forbidden line emission. Astrophys. J. **831**(2), 169 (2016). https://doi.org/10.3847/0004-637X/831/2/169. arXiv:1608.06992 [astro-ph.SR]
71. A. Banzatti, I. Pascucci, S. Edwards, M. Fang, U. Gorti, M. Flock, Kinematic links and the coevolution of MHD winds, jets, and inner disks from a high-resolution optical [OI] survey. Astrophys. J. **870**(2), 76 (2019). https://doi.org/10.3847/1538-4357/aaf1aa. arXiv:1811.06544 [astro-ph.HE]
72. M. Gangi, B. Nisini, S. Antoniucci, T. Giannini, K. Biazzo, J.M. Alcalá, A. Frasca, U. Munari, A.A. Arkharov, A. Harutyunyan, C.F. Manara, E. Rigliaco, F. Vitali, GIARPS high-resolution observations of T Tauri stars (GHOsT). II. Connecting atomic and molecular winds in protoplanetary disks. Astron. Astrophys. **643**, 32 (2020). https://doi.org/10.1051/0004-6361/202038534. arXiv:2008.01977 [astro-ph.SR]
73. C. Rab, M. Weber, T. Grassi, B. Ercolano, G. Picogna, P. Caselli, W.-F. Thi, I. Kamp, P. Woitke, Interpreting molecular hydrogen and atomic oxygen line emission of T Tauri disks with photoevaporative disk wind models. sub. to A &A (2022)
74. F. Louvet, C. Dougados, S. Cabrit, D. Mardones, F. Ménard, B. Tabone, C. Pinte, W.R.F. Dent, The HH30 edge-on T Tauri star. A rotating and precessing monopolar outflow scrutinized by ALMA. Astron. Astrophys. **618**, 120 (2018). https://doi.org/10.1051/0004-6361/201731733. arXiv:1808.03285 [astro-ph.GA]
75. O. Gressel, J.P. Ramsey, C. Brinch, R.P. Nelson, N.J. Turner, S. Bruderer, Global hydromagnetic simulations of protoplanetary disks with stellar irradiation and simplified thermochemistry. Astrophys. J. **896**(2), 126 (2020). https://doi.org/10.3847/1538-4357/ab91b7. arXiv:2005.03431 [astro-ph.EP]
76. J.E. Owen, B. Ercolano, C.J. Clarke, The imprint of photoevaporation on edge-on discs. Mon. Not. RAS **411**(2), 1104–1110 (2011). https://doi.org/10.1111/j.1365-2966.2010.17750.x. arXiv:1010.1079 [astro-ph.SR]
77. B. Ercolano, C.J. Clarke, A.C. Hall, The clearing of discs around late-type T Tauri stars: constraints from the infrared two-colour plane. Mon. Not. RAS **410**(1), 671–678 (2011). https://doi.org/10.1111/j.1365-2966.2010.17473.x. arXiv:1008.0866 [astro-ph.SR]
78. M.A. Hutchison, G. Laibe, S.T. Maddison, On the maximum grain size entrained by photoevaporative winds. Mon. Not. RAS **463**(3), 2725–2734 (2016). https://doi.org/10.1093/mnras/stw2191. arXiv:1008.0866 [astro-ph.SR]

79. M.A. Hutchison, Dusty photoevaporation in protoplanetary discs. PhD Thesis, Swinburne University of Technology, Australia (2017)
80. R. Franz, G. Picogna, B. Ercolano, T. Birnstiel, Dust entrainment in photoevaporative winds: the impact of X-rays. Astron. Astrophys. **635**, 53 (2020). https://doi.org/10.1051/0004-6361/201936615. arXiv:2001.10545 [astro-ph.EP]
81. M.A. Hutchison, C.J. Clarke, Dust delivery and entrainment in photoevaporative winds. Mon. Not. RAS **501**(1), 1127–1142 (2021). https://doi.org/10.1093/mnras/staa3608. arXiv:2011.08631 [astro-ph.EP]
82. R.A. Booth, C.J. Clarke, Modelling the delivery of dust from discs to ionized winds. Mon. Not. RAS **502**(2), 1569–1578 (2021). https://doi.org/10.1093/mnras/stab090. arXiv:2101.04121 [astro-ph.EP]
83. P.J. Rodenkirch, C.P. Dullemond, Dust entrainment in magnetically and thermally driven disk winds. Astron. Astrophys. **659**, 42 (2022). https://doi.org/10.1051/0004-6361/202142571. arXiv:2201.01478 [astro-ph.EP]
84. K.L. Luhman, P.R. Allen, C. Espaillat, L. Hartmann, N. Calvet, The disk population of the Taurus star-forming region. Astrophys. J. Suppl. **186**(1), 111–174 (2010). https://doi.org/10.1088/0067-0049/186/1/111. arXiv:0911.5457 [astro-ph.GA]
85. B. Ercolano, C. Koepferl, J. Owen, T. Robitaille, Far-infrared signatures and inner hole sizes of protoplanetary discs undergoing inside-out dust dispersal. Mon. Not. RAS **452**(4), 3689–3695 (2015). https://doi.org/10.1093/mnras/stv1528. arXiv:1507.01935 [astro-ph.EP]
86. C.M. Koepferl, B. Ercolano, J. Dale, P.S. Teixeira, T. Ratzka, L. Spezzi, Disc clearing of young stellar objects: evidence for fast inside-out dispersal. Mon. Not. RAS **428**(4), 3327–3354 (2013). https://doi.org/10.1093/mnras/sts276. arXiv:1210.6268 [astro-ph.SR]
87. G.P. Rosotti, B. Ercolano, J.E. Owen, P.J. Armitage, The interplay between X-ray photoevaporation and planet formation. Mon. Not. RAS **430**(2), 1392–1401 (2013). https://doi.org/10.1093/mnras/sts725. arXiv:1301.3015 [astro-ph.SR]
88. B. Ercolano, M.L. Weber, J.E. Owen, Accreting transition discs with large cavities created by X-ray photoevaporation in C and O depleted discs. Mon. Not. RAS **473**(1), 64–68 (2018). https://doi.org/10.1093/mnrasl/slx168. arXiv:1710.03816 [astro-ph.EP]
89. M. Gárate, T.N. Delage, J. Stadler, P. Pinilla, T. Birnstiel, S.M. Stammler, G. Picogna, B. Ercolano, R. Franz, C. Lenz, Large gaps and high accretion rates in photoevaporative transition disks with a dead zone. Astron. Astrophys. **655**, 18 (2021). https://doi.org/10.1051/0004-6361/202141444. arXiv:2110.09449 [astro-ph.EP]
90. C. Yasui, N. Kobayashi, A.T. Tokunaga, M. Saito, C. Tokoku, The lifetime of protoplanetary disks in a low-metallicity environment. Astrophys. J. **705**(1), 54–63 (2009). https://doi.org/10.1088/0004-637X/705/1/54. arXiv:0908.4026 [astro-ph.SR]
91. C. Yasui, N. Kobayashi, A.T. Tokunaga, M. Saito, C. Tokoku, Short lifetime of protoplanetary disks in low-metallicity environments. Astrophys. J. Lett. **723**(1), 113–116 (2010). https://doi.org/10.1088/2041-8205/723/1/L113. arXiv:1010.1668 [astro-ph.SR]
92. C. Yasui, N. Kobayashi, A.T. Tokunaga, M. Saito, Rapid evolution of the innermost dust disc of protoplanetary discs surrounding intermediate-mass stars. Mon. Not. RAS **442**(3), 2543–2559 (2014). https://doi.org/10.1093/mnras/stu1013. arXiv:1405.5284 [astro-ph.SR]
93. Y. Takagi, Y. Itoh, A. Arai, S. Sai, Y. Oasa, Rapid dissipation of protoplanetary disks in Ophiuchus. Publ. ASJ **67**(5), 87 (2015). https://doi.org/10.1093/pasj/psv062. arXiv:1506.04363 [astro-ph.SR]
94. B. Ercolano, D. Mayr, J.E. Owen, G. Rosotti, C.F. Manara, The dotM-M_* relation of pre-main-sequence stars: a consequence of X-ray driven disc evolution. Mon. Not. RAS **439**(1), 256–263 (2014). https://doi.org/10.1093/mnras/stt2405. arXiv:1312.3154 [astro-ph.SR]
95. A.D. Sellek, R.A. Booth, C.J. Clarke, A dusty origin for the correlation between protoplanetary disc accretion rates and dust masses. Mon. Not. RAS **498**(2), 2845–2863 (2020). https://doi.org/10.1093/mnras/staa2519. arXiv:2008.07530 [astro-ph.EP]
96. A. Somigliana, C. Toci, G. Lodato, G. Rosotti, C.F. Manara, Effects of photoevaporation on protoplanetary disc 'isochrones'. Mon. Not. RAS **492**(1), 1120–1126 (2020). https://doi.org/10.1093/mnras/stz3481. arXiv:1912.05623 [astro-ph.EP]
97. B. Tabone, G.P. Rosotti, G. Lodato, P.J. Armitage, A.J. Cridland, E.F. van Dishoeck, MHD disc winds can reproduce fast disc dispersal and the correlation between accretion rate and disc mass in Lupus. Mon. Not. RAS **512**(1), 74–79 (2022). https://doi.org/10.1093/mnrasl/slab124. arXiv:2111.14473 [astro-ph.EP]
98. L. Trapman, B. Tabone, G. Rosotti, K. Zhang, Effect of MHD wind-driven disk evolution on the observed sizes of protoplanetary disks. Astrophys. J. **926**(1), 61 (2022). https://doi.org/10.3847/1538-4357/ac3ed5. arXiv:2112.00645 [astro-ph.EP]
99. L. Wang, X.-N. Bai, J. Goodman, Global Simulations of Protoplanetary Disk Outflows with Coupled Non-ideal Magnetohydrodynamics and Consistent Thermochemistry. Astrophysical Journal **874**(1), 90 (2019). https://doi.org/10.3847/1538-4357/ab06fd. arXiv:1810.12330 [astro-ph.EP]
100. P.J. Rodenkirch, H. Klahr, C. Fendt, C.P. Dullemond, Global axisymmetric simulations of photoevaporation and magnetically driven protoplanetary disk winds. Astron. Astrophys. **633**, 21 (2020). https://doi.org/10.1051/0004-6361/201834945. arXiv:1911.04510 [astro-ph.EP]
101. R. Nakatani, T. Hosokawa, N. Yoshida, H. Nomura, R. Kuiper, Radiation Hydrodynamics simulations of photoevaporation of protoplanetary disks. II. Metallicity dependence of UV and X-ray photoevaporation. Astrophys. J. **865**(1), 75 (2018). https://doi.org/10.3847/1538-4357/aad9fd. arXiv:1805.07992 [astro-ph.EP]
102. A. Komaki, R. Nakatani, N. Yoshida, Radiation hydrodynamics simulations of protoplanetary disks: stellar mass dependence of the disk photoevaporation Rate. Astrophys. J. **910**(1), 51 (2021). https://doi.org/10.3847/1538-4357/abe2af. arXiv:2012.14852 [astro-ph.EP]